Evaluating Discrepancies Between Bulk-Rock and Single-Mineral Geochemical Data in the Magmatic Evolution of Cordilleran Arcs

Adam J. Brackman & Joshua J. Schwartz | *California State University Northridge*

Introduction

PROBLEM: Bulk-rock geochemistry has long been used as a proxy to understand the formation of plutonic rocks, but single-mineral studies at convergent margins have shown modeled equilibrium melts for these minerals deviate significantly from bulk-rock chemistry in many locations (Coint et al., 2013; Barnes et al., 2019; Brackman & Schwartz, 2021; Carty et al., 2021). The discrepancy between these two melt models raises questions about the limits of our current understanding of magma processes at convergent boundaries.

HYPOTHESIS: We hypothesize that the mismatch is due to open system behavior in magma systems whereby bulk-rock data records a history of crystal accumulation, melt expulsion and magma mixing.

Study Areas

- Two Late Cretaceous Cordilleran batholiths exposed along the paleo-Pacific margins of N. America & Zealandia:
  - Separation Point Suite (SPS), exposed on the northern tip of South Island, New Zealand and Stewart Island, New Zealand (**Fig. 1A-B**).
  - The La Posta Pluton: Large, zoned, intermediate pluton in Eastern Peninsular Ranges Batholith (E. PRB) (**Fig. 1C-D**).
- Both regions record high Sr/Y (>40), interpreted as evidence of melting of subducting oceanic slab (e.g. Defant & Drummond, 1990; Walawender et al., 1990), or melting of the deep crust within the stability field of garnet (e.g. Tulloch & Kimbrough, 2003). This ratio has been used as a proxy to estimate crustal thickness during arc emplacement (e.g. Chiaradia, 2015; Chapman et al., 2015; Profeta et al., 2015).

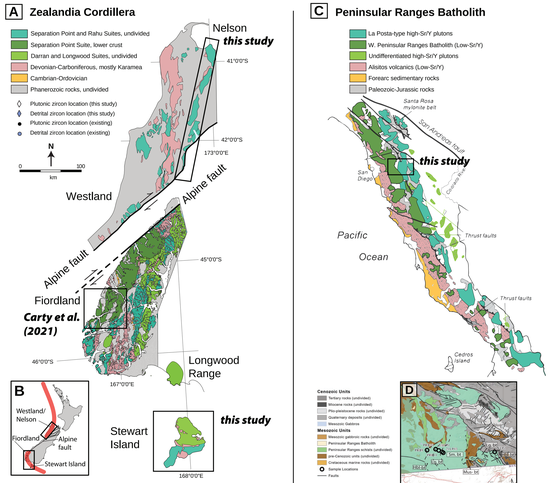

Figure 1A-D. A) Fiordland, New Zealand and igneous units of the Zealandia Cordillera. Separation Point Suite units shown in green and blue. Black boxes show extent of study area. B) Overview map of New Zealand. Deformed Median Batholith shown in red. C) Pensinsular Ranges Batholith in S. California and Baja, Mexico. Black box shows study area and extent of Fig. 1D. D) Geologic map of La Posta Pluton and surrounding units. Sample locations are marked by hollow circles and plutonic zones marked by dashed lines. Hbl-bt: hornblende-biotite facies; Lg. bt: large-biotite facies; Sm. bt: small-biotite facies; Mus-bt: muscovite-biotite facies.

Methods

- Analyzed 88 igneous amphibole grains (24 in the La Posta Pluton and 64 in Separation Point Suite)
- 1,207 40-µm spots analyzed via laser ablation sector field inductively-coupled plasma mass spectrometry (LA-SF-ICPMS) in rim-core-rim traverses for 34 trace elements.
- Corresponding 1-µm spot analyzed via electron microprobe analysis (EMPA) by the University of Alabama, at the closest distance possible to each laser pit to collect major oxide data.

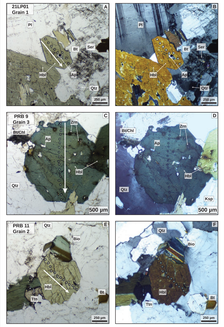

Figure 3A-F (Above Left): Representative photomicrographs of amphibole grains from the La Posta Pluton. Left column in plane-polarized light, right column in cross-polarized light.

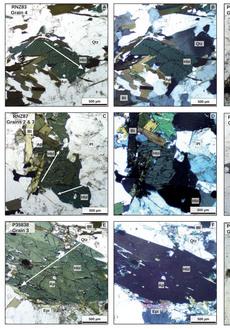

Figure 4A-F (Above Center): Amphiboles from Separation Point Suite, Westland region, Fiordland, New Zealand. White arrows in all figures show direction of analysis.

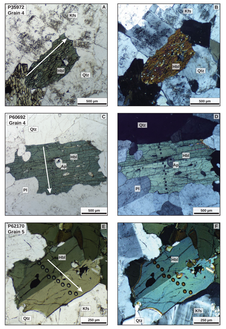

Figure 5A-F (Above Right): Representative amphiboles from Separation Point Suite, Stewart Island, New Zealand.

Bulk-Rock Compositions

Bulk-rock X-ray fluorescence (XRF) analyses from all three regions record compositions ranging from monzodiorites through granites (**Fig. 6A**).

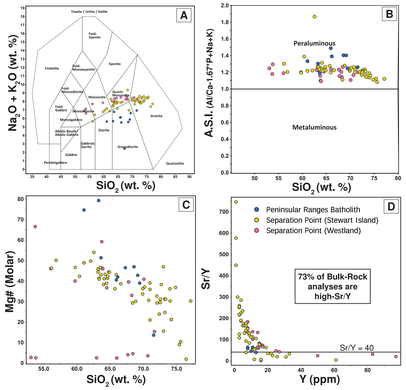

Bulk-rocks are:

- Peraluminous (**Fig. 6B**), with the majority of anlyses having ASI ranging from 1.1-1.5.
- Highly fractionated with Mg#s (molar) mostly <50 and SiO_2 ranging from 53.1 - 77.1 (wt. %) (**Fig. 6C**).
- Most analyses show high-Sr/Y (>40) (**Fig. 6D**), commonly used as a proxy to help determine crustal thicknesses during the evolution of Cordilleran arcs (e.g. Chiaradia, 2015; Chapman et al., 2015; Profeta et al., 2015) as well as evidence for melting of subducting oceanic slab or garnet-bearing lower continental crust (Defant and Drummond, 1990; Martin et al., 2005; Moyen, 2009; Chiaradia, 2015).

Figure 6A-D. 6A) Total alkali-silica (Na_2O+K_2O) vs SiO_2 (wt. %) plutonic rock classification after Middlemost, 1994. 6B) Aluminum Saturation Index (ASI) vs. SiO_2 (wt. %) after Frost and Frost, 2008. 6C) Mg# (molar) vs. bulk-rock SiO_2 (wt. %). 6D) Sr/Y vs bulk-rock Y (ppm).

Amphibole Composition & Classification

We filter our data following the methods of Werts et al., 2020, retaining 1,093/1,207 analyses. All regions show broadly similar distributions of SiO_2 (wt. %) with an apparent bimodal distribution centered around 45 and 48 % (**Fig. 7A**). All regions have similar Ca (APFU) and Al (APFU), but the bimodality is also evident in other elemental bivariate plots, with multiple compositional groups visible in all regions (**Figs. 7B, D, E**). Crystallization temperatures range from ~850-650 °C (**Fig. 7F**).

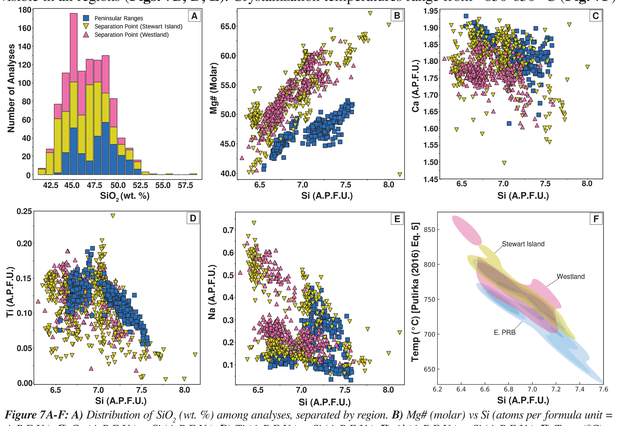

Figure 7A-F: A) Distribution of SiO_2 (wt. %) among analyses, separated by region. B) Mg# (molar) vs Si (atoms per formula unit = A.P.F.U.). C) Ca (A.P.F.U.) vs Si (A.P.F.U.). D) Ti (A.P.F.U.) vs Si (A.P.F.U.). E) Al (A.P.F.U.) vs Si (A.P.F.U.). F) Temp (°C) calculated per Putirka (2006) Equation 5 vs Si (A.P.F.U.). Contour shades indicate 25%, 50%, and 75% density.

Amphibole-Equilibrium Melt Models

- Using the chemometric equations of Zhang et al. (2017) to model major oxides, only 44.6% (488/1,093) analyses fit the calibration range (Si (APFU) < 7.0; T > 750 °C). Of these, 95/488 fall within the experimentally determined range for amphibole-melt equilibrium ($^{Fe\text{-}Mg}Kd$) (**Fig. 8A**) (Putirka, 2016).
- Samples in the equilibrium range range deviate significantly from their bulk-rock counterparts. Red lines in **Figs. 8B-F** indicate 1:1 relationship between bulk-rock and amph-melt.
- Melt trace-elements display steep light and middle REE patterns, but flat HREE slopes (**Figs. 8G-I**), suggesting these amphiboles did not form with or from a garnet-bearing reservoir.

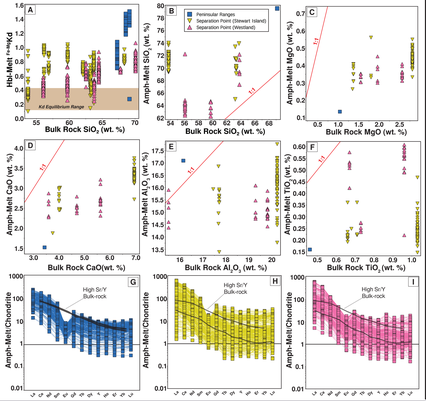

Figure 8A-I: A) Amph-Melt Fe-Mg exchange coefficient vs Bulk-rock SiO_2 (wt. %). B) Amph-melt SiO_2 (wt. %) vs Bulk-rock SiO_2 (wt. %). Red-line indicates 1:1 relationship. C) Amph-melt MgO vs Bulk-rock MgO. D) Amph-melt CaO vs Bulk-rock CaO. E) Amph-melt Al_2O_3 vs Bulk-rock Al_2O_3. F) Amph-melt TiO_2 Bulk-rock TiO_2. G-I) Amphibole-Melt/Chondrite rare earth element diagrams for each region in this study. Gray lines indicate average high-Sr/Y bulk-rock analyses.

What Does High-Sr/Y Really Mean?

- Our results suggest that the high-Sr/Y signature preserved in bulk-rock analyses is likely the result of mineral aggregation, as our melt models show both high-Sr/Y (261/1,093) and low-Sr/Y (832/1,093) signatures and are notably lacking in common evidence for garnet fractionation (**Fig 9A**).
- Dy/Dy* trends suggest a strong amphibole control on melt fractionation, driving analyses towards the origin (see inset vectors in **Fig. 9B**).
  - Consistent with other single mineral equilibrium studies (e.g. Coint et al, 2013; Barnes et al., 2019; Werts et al., 2020; Carty et al., 2021; Brackman & Schwartz, 2021).

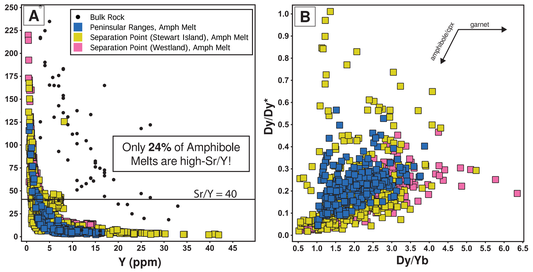

Figure 9A-B. A) Sr/Y vs Amphibole-equilibrium melt and bulk-rock Y(ppm). Bulk-rock distribution has significantly higher Sr/Y average than amphibole melts. B) Dy/Dy vs Dy/Yb. Dy/Dy* calculation and fractionation vectors after Davidson, Turner, & Plank, 2013.*

Conclusions & Future Work

- Amphibole-equilibrium melts from the La Posta Pluton in S. California and the Separation Point Suite in New Zealand do not show significant evidence of garnet control in their fractionation history, unlike bulk-rock analyses.
- The high-Sr/Y signature in bulk-rock analyses from these regions appears to be a result of plagioclase mineral aggregation, NOT a primary melt feature.
- Coupled with previous studies in the lower-crust of New Zealand (Brackman & Schwartz, 2021; Carty et al., 2021), this suggests that bulk-rock analyses from these regions are not good proxies for the original melts from which they formed.
- **Taken together, our results imply that bulk-rock analyses may be a poor proxy for melts at any depth!**
- Future work will include geobarometry and thermometry to model emplacement temperatures and pressures based on amphibole compositions.

Acknowledgements

Funding provided by the National Science Foundation (NSF) and the CSUN Hanna Graduate Fellowship program.
Special thanks to: Ian Anderson (U. of Alabama), Dr. Zhan Peng (CSUN), Gillian Greenberg, and John Wiesenfeld.

References

Barnes, C.G., Werts, K., Memeti, V., and Ardill, K., 2020. Most Granitoid Rocks are Cumulates: Deductions from Hornblende Compositions and Zircon Saturation: Journal of Petrology, v. 60, p. 2227–2240, doi:10.1093/petrology/egaa008; **Brackman, A.J. and Schwartz, J.J, 2021**, The Formation of High-Sr/Y Plutons in Cordilleran-Arc Crust by Crystal Accumulation and Melt Loss: Geosphere, *accepted*; **Carty, K., Schwartz, J.J., Klepeis, K., Stowell, H., Tulloch, A., Barnes, C.G., 2021**, The Generation of Arc Andesites and Dacites in the Lower Crust of a Cordilleran arc, Fiordland, New Zealand: Journal of Petrology, *accepted*; **Chapman, J.B., Ducea, M.N., DeCelles, P.G., and Profeta, L., 2015**, Tracking changes in crustal thickness during orogenic evolution with Sr/Y: An example from the North American Cordillera: Geology, v. 43, p. 919–922, doi:10.1130/g36996.1; **Chiaradia, M., 2015**, Crustal thickness control on Sr/Y signatures of recent arc magmas: an Earth scale perspective: Scientific Reports, v. 5, p. 8115, doi:10.1038/srep08115 ; **N. Coint, C.G. Barnes, A.S. Yoshinobu, M.A. Barnes, S. Buck**: Use of trace element abundances in augite and hornblende to determine the size, connectivity, timing, and evolution of magma batches in a tilted batholith. Geosphere 2013;; 9 (6): 1747–1765. doi: https://doi.org/10.1130/GES00931.1; **Davidson, J., Turner, S., and Plank, T., 2013**, Dy/Dy*: Variations Arising from Mantle Sources and Petrogenetic Processes: Journal of Petrology, v. 54, p. 525–537, doi:10.1093/petrology/egs076; **Frost, B.R. and Frost, C.D., 2008**, A geochemical classification for feldspathic igneous rocks. Journal of Petrology, v. 49, p. 1955-1969.; **Defant, M.J., and Drummond, M.S., 1990**, Derivation of some modern arc magmas by melting of young subducted lithosphere: Nature, v. 347, p. 662–665, doi:10.1038/347662a0.; **Leake, B.E. et al., 1997**, Nomenclature of Amphiboles; Report of the Subcommittee on Amphiboles of the International Mineralogical Association Commission on New Minerals and Mineral Names: Mineralogical Magazine, v. 61, p. 295–310, doi:10.1180/minmag.1997.061.405.13.; **Martin, H., 1999**, Adakitic magmas: modern analogues of Archaean granitoids: Lithos, v. 46, p. 411–429, doi:10.1016/s0024-4937(98)00076-0.; **Middlemost, E.A.K., 1994**, Naming materials in the magma/igneous rock system: Earth-Science Reviews, v. 37, pp. 215-224; **Moyen, J.-F., 2009**, High Sr/Y and La/Yb ratios: The meaning of the "adakitic signature": Lithos, v. 112, p. 556–574, doi:10.1016/j.lithos.2009.04.001.; **Nandedkar, R.H., Hürlimann, N., Ulmer, P., and Müntener, O., 2016**. Amphibole-melt trace element partitioning of fractionating calc-alkaline magmas in the lower crust: an experimental study. Contributions to Mineralogy and Petrology, v. 171, p. 71, doi:10.1007/s00410-016-1278-0.; **Putirka, K., 2016**. Special Collection: Rates and Depths of Magma Ascent on Earth: Amphibole thermometers and barometers for igneous systems and some implications for eruption mechanisms of felsic magmas at arc volcanoes: American Mineralogist, v. 101, p. 841–858, doi:10.2138/am-2016-5506; **Tulloch, A.J., and Kimbrough, D.L., 2003**, Paired plutonic belts in convergent margins and the development of high Sr/Y magmatism: Peninsular Ranges batholith of Baja-California and Median batholith of New Zealand: The Tectonic Evolution of Northwestern Mexico and the Southwestern USA. Geol. Soc. Amer. Spec. Paper, v. 374, p. 275–295.; **Walawender, M.J., Gastil, R.G., Clinkenbeard, J.P., McCormick, W.V., Eastman, B.G., Wernicke, R.S., Wardlaw, M.S., Gunn, S.H., and Smith, B.M., 1990**, The Nature and Origin of Cordilleran Magmatism: Geological Society of America Memoirs, p. 1–18, doi:10.1130/mem174-p1.; **Werts, K., Barnes, C.G., Memeti, V., Ratschbacher, B., Williams, D., and Paterson, S.R., 2020**, Hornblende as a tool for assessing mineral-melt equilibrium and recognition of crystal accumulation: American Mineralogist, v. 105, p. 77–91, doi:10.2138/am-2020-6972.; **Zhang, J., Humphreys, M.C.S., Cooper, G.F., Davidson, J.P., and Macpherson, C.G., 2017**, Magma mush chemistry at subduction zones, revealed by new melt major element inversion from calcic amphiboles: American Mineralogist, v. 102, p. 1353–1367, doi:10.2138/am-2017-5928.